# Nonlocality Induces Chains of Nested Dissipative Solitons

J. Javaloyes,[1] M. Marconi,[2] and M. Giudici[2]
[1]Departament de Física, Universitat de les Illes Baleares, C/Valldemossa km 7.5, 07122 Mallorca, Spain
[2]Université Côte d'Azur, CNRS, Institut de Physique de Nice, F-06560 Valbonne, France

(Received 8 November 2016; revised manuscript received 15 February 2017; published 18 July 2017)

Dissipative solitons often behave as quasiparticles, and they may form molecules characterized by well-defined bond distances. We show that pointwise nonlocality may lead to a new kind of molecule where bonds are not rigid. The elements of this molecule can shift mutually one with respect to the others while remaining linked together, in a manner similar to interlaced rings in a chain. We report experimental observations of these chains of nested dissipative solitons in a time-delayed laser system.

DOI: 10.1103/PhysRevLett.119.033904

In a seminal contribution, Turing set the bases of morphogenesis [1]. He demonstrated that, in a dissipative environment, the interplay between *local* nonlinearities and differential operators was sufficient to initiate self-organization and to generate an infinite variety of patterns. These emergent structures can be found in many physical, biological, and laboratory systems. Among them, dissipative solitons (DSs) are of particular interest, and they have been widely observed in nature [2–5]. When DSs can be individually addressed by a local perturbation, they have also been called localized structures [6–9]. These states are particularly relevant for applications when implemented in optical resonators as light bits for information processing [10–12]. Dissipative solitons may form bound states, also called "molecules," via the overlap of their oscillating tails, which creates "covalent" bonds leading to stable equilibrium distances [13–19].

In this Letter we disclose a different kind of molecule composed by chains of nested DSs, which are globally bounded yet locally independent, like an ensemble of interlaced rings. Interesting enough, similar molecular structures exist in chemistry; they are composed by interlocked macrocycles and are called catenanes [20]. While the usual covalent bound states of DSs move as a rigid ensemble when subject to perturbations, the stability analysis of these interlaced DSs reveals that they exhibit several neutral modes corresponding to the individual translation of each element. In other words, small displacements between the components do not relax, yet the ensemble remains stable. We show that these molecules, which challenge the usual notion of local stability for DS compounds, can be obtained in the presence of a pointwise nonlocality coupling a field $\Phi(x,t)$ to a distant point in space $\Phi(x+\Delta,t)$.

Nonlocality has been widely explored in spatially extended systems and has been shown to induce patterns [21], convective instabilities [22,23], or $N$-fold structures [24]. Distributed nonlocality was recently found capable of stabilizing DSs [25] and was identified as an important mechanism governing the morphogenesis processes in liquid crystal [26] and vegetation patterns [27]. Global coupling, as an extreme case of nonlocality, is known to have a deep impact on DS bifurcation diagrams [28].

Let us consider a partial differential equation (PDE) in one spatial dimension $x$ able to sustain DSs of characteristic length $l$. The difference between standard covalent molecules and the nested states can be illustrated by adding to this PDE a small pointwise nonlocal perturbation of range $\Delta$ and amplitude $\varepsilon$. We have

$$\partial_t \Phi = \mathcal{F}(|\Phi|^2, \partial_x^2)\Phi + \varepsilon \Phi(x+\Delta, t), \qquad (1)$$

where $\mathcal{F}$ is a generic operator which may lead, for example, to the Ginzburg-Landau equation, as in Ref. [2]. For sufficiently small values of $\varepsilon$, the overall structure of the unperturbed DS solution is preserved, but it develops a small echo of amplitude $\varepsilon$ at the distance $\Delta$, as a consequence of the nonlocal term. This is qualitatively shown in Fig. 1(a), where we assumed that $\Delta > 0$. Because of the nonlocal term, additional weaker replicas of this echo also appear at distances $n\Delta$ ($n \in \mathbb{N}$), with amplitudes $\varepsilon^n$, but they can be neglected in this discussion. Without the nonlocal term ($\varepsilon = 0$), standard covalent molecules are generated by an interaction between the decaying oscillating tails of two nearby DSs, thus leading to equilibrium distances $d \sim l$, as in Refs. [16,17]. When $\varepsilon \neq 0$, and for nonlocality range $\Delta \sim l$, the rightmost DS tail will be

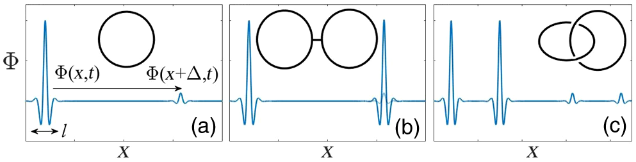

FIG. 1. (a) Sketch of a DS with a pointwise nonlocal term Δ. (b) Covalent molecule where the rightmost DS is linked to the leftmost one via its echo. Note that the echo of the rightmost DS falls outside the panel. (c) Molecule with nested elements.

modified, which may induce additional equilibrium distances. In this case, the binding occurs as a consequence of the interaction between the main pulse of a second DS and the echo of the first, which induces an equilibrium distance $d \sim \Delta$, that is robust even when $\Delta \gg l$, as shown in Fig. 1(b). All these molecules are rigid since they feature well-determined bond lengths and they exhibit a single neutral mode corresponding to the translation degree of freedom of the whole ensemble. A novel kind of molecule appears in the case $\Delta \gg l$, when the second DS is placed at a distance $d$ from the first DS such that $l < d < \Delta$. In this case, shown in Fig. 1(c), the two DSs are sufficiently far so that they can move independently but, at the same time, the second DS cannot overcome the repulsive barrier induced by the echo of the first DS. As such, the two DSs are globally linked while being locally independent. A useful analogy to picture these situations can be made using rings which are rigidly bound in the situation represented in Fig. 1(b), while they are interlaced in the case of Fig. 1(c).

Pointwise nonlocality may not be easy to achieve experimentally and, in order to observe such new bounded states, we have studied their realization in time-delayed systems (TDSs). In recent years, building on the strong analogies between spatially extended and time-delayed systems [29–31], the latter have been proposed for controlling spatial DSs [32], hosting chimera states [33], domain walls [34–36], vortices [37], and, in particular, temporal DSs [38–42]; see Ref. [43] for a review. The idea that a feedback with a time delay $\tau_f$ is akin to a spatial dimension is rooted in the representation developed in Ref. [29] based on the observation that TDSs exhibit slowly evolving periodic regimes with period $T \sim \tau_f$. By cutting the temporal trace generated by a TDS into $n \in \mathbb{N}$ chunks of duration $T$ and stacking them into a two-dimensional map, one obtains a diagram in which the horizontal dimension plays the role of a pseudospatial variable representing the waveform within the $n$th period, while the vertical axis depicts the discrete time index $n$. In this formalism [30], the temporal profile over one period—the information in pseudospace—is mapped onto the next period. As such, one understands that the inclusion of a perturbation with a second delay $\tau_r$ induces a pointwise nonlocality with range $\Delta = \tau_r$. If the temporal profile does not evolve significantly during $p$ periods, similar results are to be found whenever $\tau_r = pT + \Delta$. We conclude that the effective nonlocal parameter $\Delta$ is $\Delta = \tau_r[T]$, with $[\cdot]$ being the modulo operator.

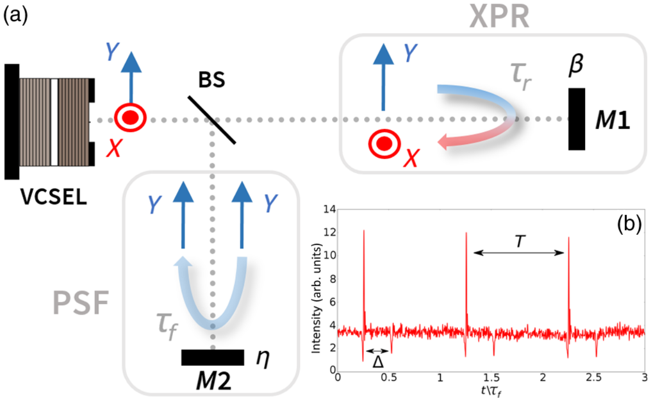

FIG. 2. (a) Double delay experimental situation featuring DSs with nonlocal coupling. VCSEL output is split into two arms by a beam splitter (BS). Along the first (polarization selective feedback, PSF), $Y$ polarization is selected, and it is fed back after a delay $\tau_f$ at a rate $\eta$. Along the second (crossed polarization reinjection, XPR), $Y$ polarization is selected, rotated into the orthogonal polarization direction ($X$) and reinjected after a delay $\tau_r$ at a rate $\beta$. (b) Experimental time trace of the $X$ polarization intensity showing a single DS per period.

An example of a photonic system with a double time delay capable of hosting DSs and molecules has recently been described [41] and is summarized in Fig. 2(a). A single-transverse mode vertical-cavity surface-emitting laser (VCSEL) is coupled to an external cavity that selects one of the linearly polarized states of the VCSEL ($Y$, say) and feeds it back twice, once with a time delay $\tau_f$, and once with a delay $\tau_r$ after being rotated into the orthogonal direction. Experimental results described in Ref. [41], show that, when $\tau_f$ is much larger than the laser time scales, this system may host vectorial DSs which correspond to a full rotation of the polarization vector state on the Poincaré sphere, mainly along its equatorial plane. Accordingly, the $X$ polarization component of these DSs corresponds to upward pulses over a low intensity background [Fig. 2(b)], while their $Y$ polarization is in perfect antiphase with $X$, thus leaving the total intensity constant. Figure 2(b) shows that the main pulse corresponding to the $X$ component of the DS is followed by a small inverted kink after a time $\Delta$. This echo is the signature of the nonlocal coupling described in Fig. 1(a), induced here by the additional delay $\tau_r$, which leads to a nonlocality range $\Delta$. It is worth noting that this observation is reminiscent of the interaction between temporal DSs in injected Kerr fibers mediated by sound waves [44], although, in our case, the effect is fully controllable and can be used to tune the interaction between DSs. As illustrated in Fig. 1(b), the echoes observed in Fig. 2(b) create binding forces leading to the existence of molecules whose separation between elements $d$ is precisely $d = \Delta$ or integer multiples of $\Delta$. Several of these covalent molecules have been experimentally reported in Ref. [41] for short nonlocal range $\Delta \simeq l$.

These observations are well described by the so-called spin-flip model [45], supplemented by the inclusion of the delayed reinjection terms. A multiple time scales analysis of this model applied in the limit of large damping of the relaxation oscillations, negligible dichroism, moderate birefringence $\gamma_p$, and feedback rates $(\eta, \beta)$ leads to a simple equation describing the azimuthal angle $\Phi$ of the polarization vector over the equatorial plane of the Poincaré sphere [41,46]. The following simpler delayed equation was found to reproduce well the dynamics:

$$\frac{\dot{\Phi}}{2} = \alpha\gamma_p \sin\Phi + \bar{\eta}\sin\frac{\Phi^{\tau_f}}{2}\cos\frac{\Phi}{2} - \bar{\beta}\sin\frac{\Phi}{2}\sin\frac{\Phi^{\tau_r}}{2}, \qquad (2)$$

with $\Phi^{\tau_{f,r}} = \Phi(t-\tau_{f,r})$ being the delayed arguments, $(\bar{\eta},\bar{\beta}) = (\eta,\beta)\sqrt{1+\alpha^2}$, with $\alpha$ being the Henry's linewidth enhancement factor. If not otherwise stated, the parameters are $\alpha = 2$, $\gamma_p/\pi = 4.78$ GHz, $\eta/\pi = 8.68$ GHz, $\beta/\pi = 6.68$ GHz, $\tau_f = 3.33$ ns, and $\tau_r = 4$ ns. Assuming a constant intensity $I_0$, the $X$ and $Y$ components of the intensity read $I_x = \cos^2(\Phi/2)$ and $I_y = I_0\sin^2(\Phi/2)$. However, linearly polarized light can have arbitrary orientations that are neither $X$ nor $Y$. This is taken into account by defining the normalized Stoke parameters along the equator $S_1 = \cos(\Phi)$ and $S_2 = \sin(\Phi)$.

Equation (2) is used for exploring the situation where $\Delta \gg l$ and, in Figs. 3(a) and 3(c), a typical covalent molecule of DSs is depicted in terms of the Stokes parameters and the polarization resolved intensities. Each element of the molecule is composed by a large polarization kink for $\Phi$ followed by its nonlocal echo at a distance $\Delta$, and the echo of the first DS is the anchor point for the second. In addition to these covalent structures, which exemplify the situation shown in Fig. 1(b), a novel kind of molecules is observed where the elements are interlaced one with another, as sketched in Fig. 1(c). An example of these nested DS molecules where the second DS is trapped between the first DS and its echo is described in Figs. 3(b) and 3(d). Figure 3(b) shows that, on the Poincaré sphere, the molecule is defined by a large rotation of the polarization vector corresponding to the main peak of the first DS. This is followed by opposite rotation corresponding to the main peak of the second DS, thus bringing back the vector to the original state. Similar but smaller kinks follow corresponding to the nonlocal echoes of the two DSs. Accordingly, Fig. 3(b) evidences that this nested molecule has the additional property of being a kink-antikink pair, such that the total topological charge is zero.

Considering the DSs as periodic solutions of a high-dimensional dynamical system permitted us to perform the analysis of their Floquet multipliers. Floquet theory allows us to study the linear stability of periodic solutions; see, for instance, Ref. [47]. The stability analysis performed in Ref. [41] confirmed that the covalent molecule in Figs. 3(a) and 3(c) possesses a single neutral mode corresponding to the translation invariance of the whole molecule. The results of a similar analysis applied to the nested molecule in Figs. 3(b) and 3(d) are summarized in Fig. 4. The temporal profile of the solution over which we performed the stability analysis is depicted in Fig. 4(a), and one notices in Fig. 4(b) not one but *two* quasidegenerate Floquet multipliers $\mu_i$ close to the value $\mu = 1$ in the complex plane. We also show in Fig. 4(a) the eigenvectors associated with these two neutral modes. One can easily identify them with the temporal derivatives of the kink and of the antikink composing the nested molecule, which

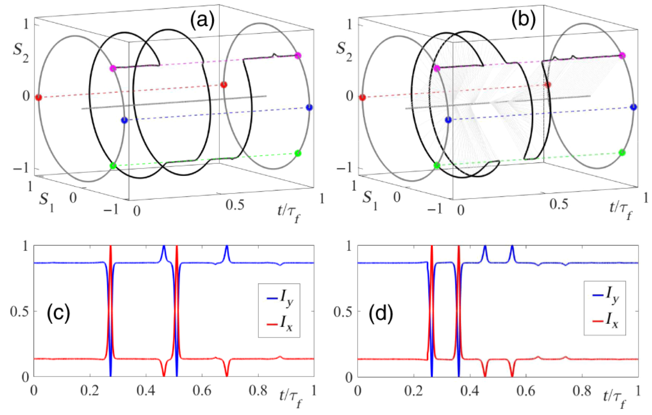

FIG. 3. Numerical integration of Eq. (2). Evolution of the Stokes parameters $(S_1, S_2)$ and intensities $(I_x, I_y)$ in the cases of (a),(c) a covalent and (b),(d) a catenane molecule. Pure emission along the $X$ and $Y$ directions correspond to the red and blue lines with $(S_1, S_2) = (1, 0)$ and $(S_1, S_2) = (-1, 0)$, respectively. The steady state of Eq. (2), $\Phi_s$, is depicted in pink, while the green line represents $-\Phi_s$.

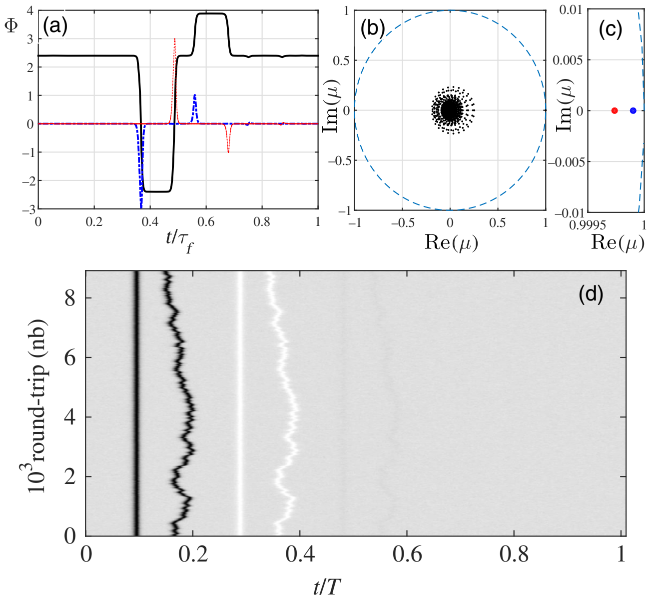

FIG. 4. Numerical analysis of the catenane molecule in Figs. 3(b) and 3(d). (a) Temporal profile (black line) and the associated neutral eigenvectors (dotted blue and dashed-dotted red lines). (b) Floquet multipliers $\mu_i$ and (c) an enlargement around $\mu_i = 1$ where one distinguishes two quasidegenerate multipliers. (d) Space-time diagram of $I_x$ in the presence of additive white noise of amplitude $\xi = 3 \times 10^{-2}$. The position of each DS is given by the strong intensity peak, followed by the smaller intensity dip echoing at distance $\Delta$. The intensity of $I_x$ grows from white to black.

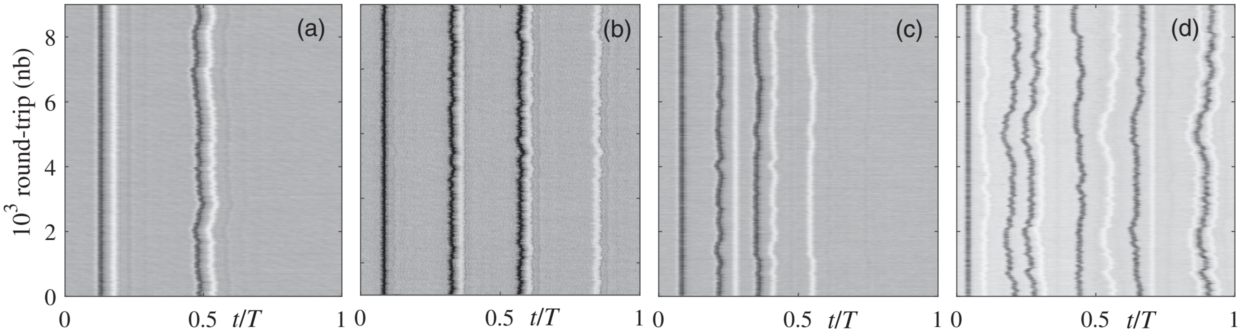

FIG. 5. Experimental space-time diagrams taking the first DS as a time reference for visually enhancing the relative motion of other DSs. In all of the cases, the bias current is $J = 10J_{\mathrm{th}}$ and $T \sim \tau_f = 10.8$ ns. (a) Two independent DSs, $\Delta = 0.68$ ns ($0.06T$). (b) Covalent molecule with $\Delta = 3.05$ ns ($0.28T$) and where the binding occurs via the interaction with the nonlocal echo. (c),(d) Two different cases of catenane molecules with (c) $\Delta = 2.08$ ns ($0.19T$) and (d) $\Delta = 7.2$ ns ($0.67T$). The intensity of $I_x$ grows from white to black.

correspond to their individual translation modes. The residual interactions between DSs, which are always present if their separation is finite, renormalize the Floquet multipliers and explain their small deviation with respect to unity. In the limit $\tau_{f,r} \to \infty$, we find numerically that they converge to $\mu = 1$. In other words, our local analysis shows that the two DSs composing the molecule are indeed locally independent. However, it fails to show their global dependence, for which the consideration of the whole temporal profile is needed.

The local independence of the DSs forming the bound state shown in Figs. 3(b) and 3(d) contrasts with the rigid behavior of the components of the covalent molecule shown in Figs. 3(a) and 3(c). This evidence is further supported by analyzing the motion of the structure represented in Fig. 3(b) and 3(d) over many round-trips in the presence of noise. While independent DSs exhibit uncorrelated random walks under the action of noise present in the system, DSs forming covalent molecules behave as a unique rigid body; see, for instance, Figs. 3(a) and 3(b) in Ref. [41]. The stochastic evolution of the nested DS molecules described in Figs. 3(b) and 3(d) is shown in Fig. 4(d) by using a spatiotemporal diagram where the time trace for the polarization resolved intensity $I_x$ is folded over itself in such a way that the first DS remains motionless. This reference frame choice permits us to better visualize the fluctuations of the distance between the components of the molecule, although it hides the Brownian evolution of the whole molecule. We stress that, because we are plotting the intensity along the $X$ direction $I_x$, the DS main pulse corresponds to a peak ($P$), while the echo corresponds to small dip ($D$) at a distance $\Delta$ from the peak. Figure 4(d) shows that, despite the fact that the two DSs can drift with respect to one another, the distance between them remains bounded, and the main kink of the second DS is always caught between the main kink of the first DS and its echo. Also, this representation allows us to distinguish morphologically two elements of a catenane molecule from two independent DSs. The signature of the first corresponds to two peaks followed by two dips—i.e., $P_1P_2D_1D_2$ in Fig. 4(d)—while two independent DSs would correspond to $P_1D_1P_2D_2$.

Our theoretical predictions of the existence of catenane molecules are supported by experimental observations. A wealth of these molecule states coexisting for the same parameter values has been observed in the experimental system described in Fig. 2(a). In Fig. 5 we plot experimentally obtained spatiotemporal diagrams using the reference frame of the leftmost DS, as in Fig. 4(d). We show the evolution of two independent DSs in Fig. 5(a) and the evolution of a standard covalent molecule, observed for large values of $\Delta$ in Fig. 5(b). Here, the binding occurs via the nonlocal echo, as in Figs. 3(a) and 3(c). Molecules of nested DSs are shown in Figs. 5(c) and 5(d). Besides the simplest catenane corresponding to $P_1P_2D_1D_2$ (not shown), we depict in Fig. 5(c) a situation where three DSs are interlaced, giving the structures $P_1P_2D_1P_3D_2D_3$. Their local independence can be deduced from their relative uncorrelated motion, similar to that of the independent DSs depicted in Fig. 5(a). Counting from left to right, we note that $\mathrm{DS}_2$ is interlaced with $\mathrm{DS}_1$, while $\mathrm{DS}_3$ is interlaced with $\mathrm{DS}_2$. A more complex catenane of six elements is shown in Fig. 5(d). Here, two elements ($\mathrm{DS}_2$ and $\mathrm{DS}_3$) are very close to each other, and their echoes trap a distant element ($\mathrm{DS}_6$) driving its diffusion, thus evidencing the binding forces induced by the echo at the source of the catenane molecules. The periodic boundary conditions in the space-time diagrams are inherent to the periodicity of the temporal traces. This explains why the rightmost DSs have their satellites on the left in Fig. 5(d).

In conclusion, we described how the presence of a pointwise nonlocality in an extended system can give rise to a new kind of molecule of DSs whose elements are simultaneously locally independent and globally locked. Owing to the strong link between spatially extended and delayed systems, we analyzed the implementation of pointwise nonlocality using a VCSEL enclosed in a double external cavity. The experimental signature of the optical catenane is found to closely match our predictions. We note that other TDSs capable of generating DSs, as in Refs. [38,39], would yield similar catenane molecules.

J. J. acknowledges the financial support from the project COMBINA (TEC2015-65212-C3-3-P MINECO/FEDER UE) and the Ramón y Cajal fellowship. M. M. and M. G. acknowledge the Universitat de les Illes Balears for the visiting positions, which enabled development of this work.

---

[1] A. M. Turing, Phil. Trans. R. Soc. A **237**, 37 (1952).
[2] S. Fauve and O. Thual, Phys. Rev. Lett. **64**, 282 (1990).
[3] *Dissipative Solitons*, edited by N. Akhmediev and A. Ankiewicz, Lecture Notes in Physics Vol. 661 (Springer, Berlin, 2005).
[4] *Dissipative Solitons: From Optics to Biology and Medicine*, edited by N. Akhmediev and A. Ankiewicz, Lecture Notes in Physics Vol. 751 (Springer, Berlin, 2008).
[5] P. Grelu and N. Akhmediev, Nat. Photonics **6**, 84 (2012).
[6] P. Coullet, C. Riera, and C. Tresser, Phys. Rev. Lett. **84**, 3069 (2000).
[7] N. N. Rosanov and G. V. Khodova, Opt. Spectrosc. **65**, 449 (1988).
[8] M. Tlidi, P. Mandel, and R. Lefever, Phys. Rev. Lett. **73**, 640 (1994).
[9] W. J. Firth and A. J. Scroggie, Phys. Rev. Lett. **76**, 1623 (1996).
[10] L. A. Lugiato, IEEE J. Quantum Electron. **39**, 193 (2003).
[11] S. Barland, J. R. Tredicce, M. Brambilla, L. A. Lugiato, S. Balle, M. Giudici, T. Maggipinto, L. Spinelli, G. Tissoni, T. Knödl, M. Miller, and R. Jäger, Nature (London) **419**, 699 (2002).
[12] F. Leo, S. Coen, P. Kockaert, S. P. Gorza, P. Emplit, and M. Haelterman, Nat. Photonics **4**, 471 (2010).
[13] N. N. Rosanov and G. V. Khodova, J. Opt. Soc. Am. B **7**, 1057 (1990).
[14] B. A. Malomed, Phys. Rev. A **44**, 6954 (1991).
[15] D. Y. Tang, W. S. Man, H. Y. Tam, and P. D. Drummond, Phys. Rev. A **64**, 033814 (2001).
[16] J. M. McSloy, W. J. Firth, G. K. Harkness, and G.-L. Oppo, Phys. Rev. E **66**, 046606 (2002).
[17] P. L. Ramazza, E. Benkler, U. Bortolozzo, S. Boccaletti, S. Ducci, and F. T. Arecchi, Phys. Rev. E **65**, 066204 (2002).
[18] P. Grelu and J. Soto-Crespo, in *Dissipative Solitons: From Optics to Biology and Medicine*, edited by N. Akhmediev and A. Ankiewicz, Lecture Notes in Physics Vol. 751 (Springer, Berlin, 2008), p. 1.
[19] V. Tsatourian, S. V. Sergeyev, C. Mou, A. Rozhin, V. Mikhailov, B. Rabin, P. S. Westbrook, and S. K. Turitsyn, Sci. Rep. **3**, 3154 (2013).
[20] H. L. Frisch and E. Wasserman, J. Am. Chem. Soc. **83**, 3789 (1961).
[21] P. L. Ramazza, S. Ducci, and F. T. Arecchi, Phys. Rev. Lett. **81**, 4128 (1998).
[22] F. Papoff and R. Zambrini, Phys. Rev. Lett. **94**, 243903 (2005).
[23] R. Zambrini and F. Papoff, Phys. Rev. Lett. **99**, 063907 (2007).
[24] S. Residori, T. Nagaya, and A. Petrossian, Europhys. Lett. **63**, 531 (2003).
[25] C. Fernandez-Oto, M. G. Clerc, D. Escaff, and M. Tlidi, Phys. Rev. Lett. **110**, 174101 (2013).
[26] M. Tlidi, C. Fernandez-Oto, M. G. Clerc, D. Escaff, and P. Kockaert, Phys. Rev. A **92**, 053838 (2015).
[27] D. Escaff, C. Fernandez-Oto, M. G. Clerc, and M. Tlidi, Phys. Rev. E **91**, 022924 (2015).
[28] W. J. Firth, L. Columbo, and A. J. Scroggie, Phys. Rev. Lett. **99**, 104503 (2007).
[29] F. T. Arecchi, G. Giacomelli, A. Lapucci, and R. Meucci, Phys. Rev. A **45**, R4225 (1992).
[30] G. Giacomelli and A. Politi, Phys. Rev. Lett. **76**, 2686 (1996).
[31] S. A. Kashchenko, Comput. Math. Math. Phys. **38**, 1 (1998).
[32] S. V. Gurevich, Phys. Rev. E **87**, 052922 (2013).
[33] L. Larger, B. Penkovsky, and Y. Maistrenko, Phys. Rev. Lett. **111**, 054103 (2013).
[34] G. Giacomelli, F. Marino, M. A. Zaks, and S. Yanchuk, Europhys. Lett. **99**, 58005 (2012).
[35] F. Marino, G. Giacomelli, and S. Barland, Phys. Rev. Lett. **112**, 103901 (2014).
[36] J. Javaloyes, T. Ackemann, and A. Hurtado, Phys. Rev. Lett. **115**, 203901 (2015).
[37] S. Yanchuk and G. Giacomelli, Phys. Rev. Lett. **112**, 174103 (2014).
[38] M. Marconi, J. Javaloyes, S. Balle, and M. Giudici, Phys. Rev. Lett. **112**, 223901 (2014).
[39] B. Garbin, J. Javaloyes, G. Tissoni, and S. Barland, Nat. Commun. **6**, 5915 (2015).
[40] B. Romeira, R. Avó, José M. L. Figueiredo, S. Barland, and J. Javaloyes, Sci. Rep. **6**, 19510 (2016).
[41] M. Marconi, J. Javaloyes, S. Barland, S. Balle, and M. Giudici, Nat. Photonics **9**, 450 (2015).
[42] J. Javaloyes, Phys. Rev. Lett. **116**, 043901 (2016).
[43] S. Yanchuk and G. Giacomelli, J. Phys. A **50**, 103001 (2017).
[44] J. K. Jang, M. Erkintalo, S. G. Murdoch, and S. Coen, Nat. Photonics **7**, 657 (2013).
[45] M. San Miguel, Q. Feng, and J. V. Moloney, Phys. Rev. A **52**, 1728 (1995).
[46] J. Javaloyes, M. Marconi, and M. Giudici, Phys. Rev. A **90**, 023838 (2014).
[47] C. A. Klausmeier, Theor. Ecol. **1**, 153 (2008).